

## A Novel Process for Oxynitride by Post-Oxidation of NH<sub>3</sub> Plasma Nitridation

Chao Sung Lai and Kung Ming Fan

Department of Electronic Engineering, Chang Gung University  
259 Wen-Hwa 1st Road, Kwei-Shan, Tao-Yuan, Taiwan

Tel: +886-3-2118800 ext 5786 Fax: +886-3-2118507 e-mail: cslai@mail.cgu.edu.tw

### Introduction

For lower power consumption, higher speed and circuit stability, multiple-thickness for gate oxide ( $T_{ox}$ ) is necessary for the system-on-a-chip (SOC) devices [1]. In this study, NH<sub>3</sub> plasma process was used for nitridation of silicon [2], and an ultra-thin nitride layer (~13Å) would be formed after NH<sub>3</sub> plasma treatment. A Novel process was developed for gate oxynitride by post-oxidation on the NH<sub>3</sub> plasma treatment substrate. The reliability was improved by increasing the post-oxidation time, including the less trap densities, better SILC immunity, lower charge trapping and higher  $Q_{bd}$ . This novel process makes the multiple  $T_{ox}$  possible and easy implements to SOC process integration.

### Experiments

Metal/oxide/silicon (MOS) capacitors were fabricated in this work. First of all, the NH<sub>3</sub> plasma nitridation effects were studied. Secondly, rapid thermal (RT) N<sub>2</sub>O post-oxidation was performed to compare with O<sub>2</sub> post-oxidation. Finally, A physical model was proposed for the post-oxidation of NH<sub>3</sub> plasma nitridation. The key processes for the NH<sub>3</sub> plasma nitridation were shown in Fig. 1 (a) O<sub>2</sub> and (b) RT N<sub>2</sub>O post-oxidation, respectively. The NH<sub>3</sub> plasma was generated by ratio frequency.

### Results and Discussion

#### *Physical Model for Post-Oxidation of NH<sub>3</sub> Plasma Nitridation*

A physical model for the post-oxidation of NH<sub>3</sub> plasma nitridation was schematic as shown in Fig. 2. The NH<sub>3</sub> plasma processed surface forms a nitride thin film and results in low oxidation growth rate. This process makes the multiple-thickness process possible and easy to implement to SOC process integration.

#### *NH<sub>3</sub> Plasma Nitridation Effects*

The NH<sub>3</sub> plasma nitridation effects on gate oxide thickness, nitrogen distribution, and electrical properties were systematic studied. Figure 3 shows the gate oxide thickness for all samples with different plasma exposure time. It can be seen that a significant difference of oxidation growth rate affected by plasma nitridation. The growth rate can be reduced 80% for the sample with NH<sub>3</sub> plasma treated 5 min. This process makes the multiple-thickness-gate-oxides possible. It could be due to the nitrogen-plasma radical (N<sup>\*</sup>) to form a nitride layer with silicon substrate, and retard the oxidation rate. The SIMS depth profiles of nitrogen, oxygen and aluminum were shown in Fig. 4. The silicon surface was treated by NH<sub>3</sub> plasma and post oxidized in O<sub>2</sub>. It shows that the nitrogen accumulated at the Si/SiO<sub>2</sub> interface and broadened into silicon-bulk.

The F-N tunneling current characteristics are shown in Fig. 5. For the thin oxide, it can be seen that a higher leakage current in the low voltage regime. It was due to direct tunneling. The leakage current is low enough for application to DRAM capacitors. The breakdown field is higher as decreasing the thickness as shown in Fig. 6.

The energy released in the thinner oxide was much less due to charge direct tunneling. It shows in Fig. 7, the gate voltage shift,  $\Delta V_g$ , under a constant current of -10 mA/cm<sup>2</sup> stressing. The gate voltage shift is much smaller, small charge trapping rate, for the NH<sub>3</sub> pretreated sample. The nitrogen incorporation terminated dangling bond in the oxide/silicon interface. The plasma damages were annihilated due to the post oxidation procedures.

#### *Post Rapid Thermal N<sub>2</sub>O Oxidation Effects*

Figure 8 shows the oxide thickness for samples with and without NH<sub>3</sub> plasma 5 min versus RT N<sub>2</sub>O oxidation time. The thickness of sample with plasma 5 min is 13Å. It was similar to the silicon nitride layer, which refractive index was in the range of 1.68~1.99. The nitrogen depth SIMS profile was shown for RT N<sub>2</sub>O oxidation sample with and without NH<sub>3</sub> plasma, respectively as shown in Fig. 9. NH<sub>3</sub> plasma process would lead to about one order higher nitrogen concentration compare to the control sample. As shown in Fig. 8, the thickness of plasma samples is 33Å and 36Å with RT N<sub>2</sub>O re-oxidation for 30 and 60 sec, respectively. We can conclude that the nitrogen introduced by NH<sub>3</sub> plasma dominated the oxide growth rate rather than RT N<sub>2</sub>O re-oxidation.

The oxide breakdown electric field was shown in Fig. 10 for NH<sub>3</sub> plasma samples with RT N<sub>2</sub>O processes. It showed that a better oxide reliability for the longer re-oxidation. It was due to the higher nitrogen redistribution and plasma damage removal by the following RT N<sub>2</sub>O thermal cycle. It's consistent for the hysteresis characteristics of C-V curves as shown in Fig. 11. The stress-induced-leakage-current (SILC) was shown in Fig. 12 for RT N<sub>2</sub>O samples (a) with and (b) without NH<sub>3</sub> plasma nitridation, respectively. The stress condition was -10 mA/cm<sup>2</sup>. For the RT N<sub>2</sub>O sample with NH<sub>3</sub> plasma nitridation, there was no SILC but for the conventional RT N<sub>2</sub>O sample, leakage current increasing. This indicated that the plasma sample has stronger SILC immunity due to the higher nitrogen concentration. Figure 13 shows the gate voltage shift under constant gate injection current, -10 mA/cm<sup>2</sup>. Longer the RT N<sub>2</sub>O re-oxidation, lower the charge trapping and higher charge to soft-breakdown were.

### Conclusions

A novel re-oxidation of NH<sub>3</sub> plasma nitridation process was proposed which obtain different oxide thickness by controlling the NH<sub>3</sub> plasma exposing time. The trap generation rate and bulk trap density was decreasing by increasing NH<sub>3</sub> plasma exposure. The oxide reliability for NH<sub>3</sub> plasma processed sample was improved by increasing the RT N<sub>2</sub>O re-oxidation time, including the less bulk trap densities, better SILC immunity, lower charge trapping rate and higher  $Q_{bd}$ .

#### **Acknowledgements**

This work was supported by the national-science-council of R. O. C. through research contract NSC 91-2215-E-182-004.

#### **References**

- [1] C. T. Liu, et al., *IEDM Tech. Dig.*, 1998, pp. 589-592.
- [2] Chao Sung Lai, et al., *IEEE Trans. on Electron Devices*, vol.43, 1996.

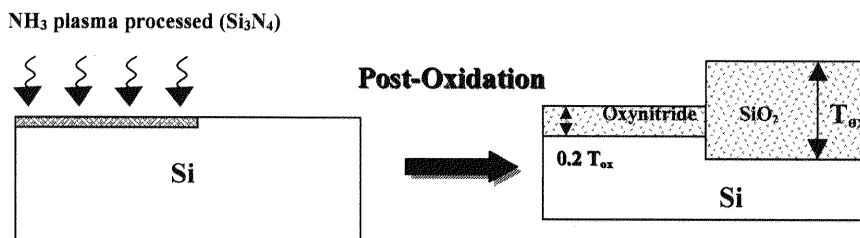
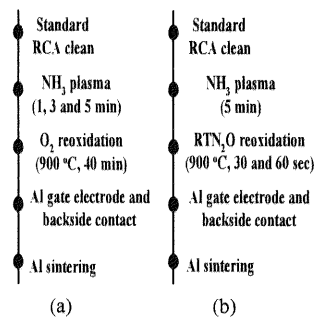


Fig.1. The key processes for the NH<sub>3</sub> plasma nitridation were shown in (a) O<sub>2</sub> and (b) RT N<sub>2</sub>O post-oxidation, respectively.

Fig.2. Physical model for the post-oxidation of NH<sub>3</sub> plasma nitridation. The difference of oxide thickness between NH<sub>3</sub> plasma pre-treated oxynitride and SiO<sub>2</sub> films are about 80% .

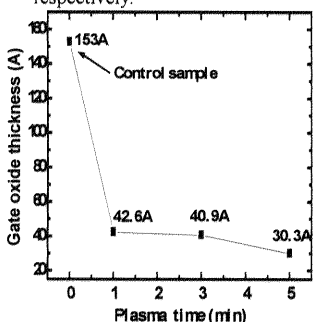


Fig.3. Gate oxide thickness measured by ellipsometer for control sample and NH<sub>3</sub> plasma pretreated samples with exposed time of 1 min, 3 min and 5 min, respectively (NH<sub>3</sub> plasma + O<sub>2</sub> re-oxidation).

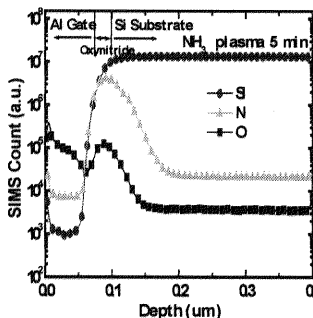


Fig.4. The SIMS depth profile of MOS structure with gate dielectric pre-treated by NH<sub>3</sub> plasma 5 min.

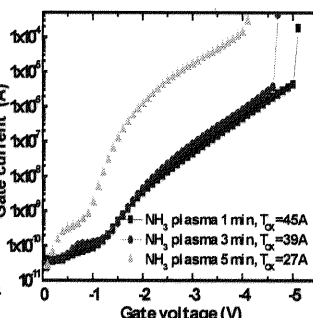


Fig. 5. The characteristic of I-V curves for different plasma exposed time. The oxide thickness was determined by C-V measurement.

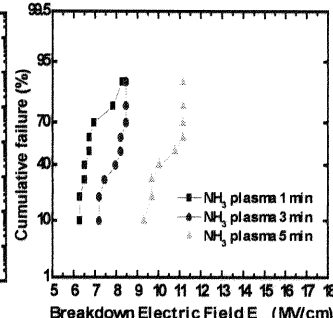


Fig.6. Cumulative plots of breakdown electric field for different NH<sub>3</sub> plasma pre-treated time.

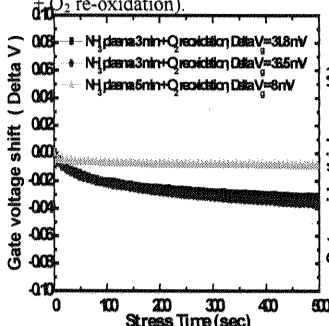


Fig.7. Plot of gate voltage shift under constant current stress at  $J = -10 \text{ mA/cm}^2$  for different NH<sub>3</sub> plasma pre-treated time.  $\Delta V_g = V_g(t) - V_g(t=0)$ .

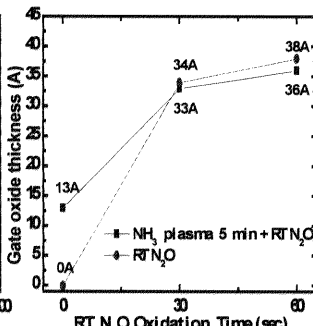


Fig.8. Gate oxide thickness for conventional RT N<sub>2</sub>O oxidation and NH<sub>3</sub> plasma pre-treated RT N<sub>2</sub>O oxidation as a function of oxidation times.

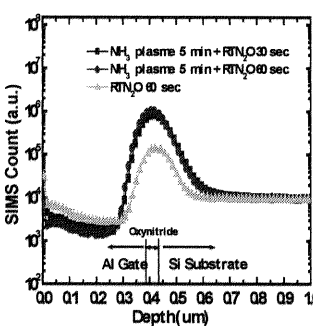


Fig.9. The SIMS depth profile for NH<sub>3</sub> plasma pre-treated and control sample with RT N<sub>2</sub>O oxidation.

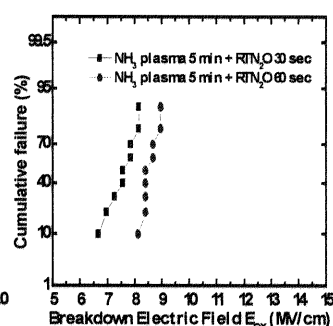


Fig.10. Cumulative plots of breakdown electric field for different RT N<sub>2</sub>O re-oxidation time.

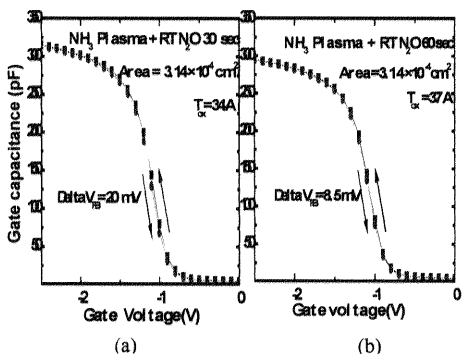


Fig.11. The hysteresis characteristics of high-frequency C-V curves for RT N<sub>2</sub>O re-oxidation with NH<sub>3</sub> plasma pre-treated for (a) 30 and (b) 60 sec, respectively.

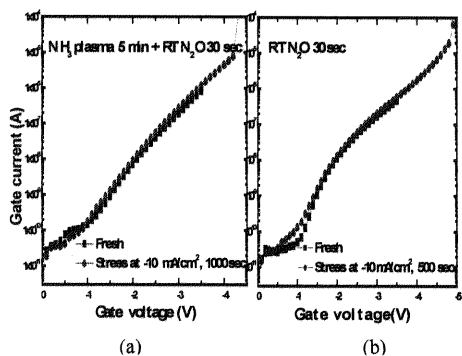


Fig.12. The SILC characteristics for (a) RT N<sub>2</sub>O re-oxidation with NH<sub>3</sub> plasma pre-treatment, stressing for 1000 sec and (b) conventional RT N<sub>2</sub>O sample, stressing for 500 sec under constant current stress at  $J_{\text{stress}} = -10 \text{ mA/cm}^2$  .

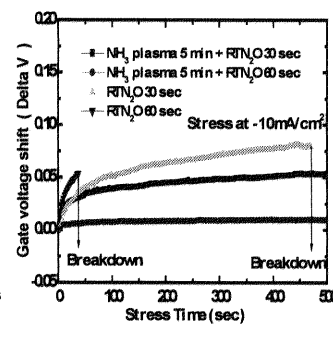


Fig.13. Gate voltage shift under constant current stress at  $J_{\text{stress}} = -10 \text{ mA/cm}^2$  for conventional RT N<sub>2</sub>O and RT N<sub>2</sub>O re-oxidation with NH<sub>3</sub> plasma pre-treatment.